

Functionality of Disorder in Muscle Mechanics

Hudson Borja da Rocha^{1,2,*} and Lev Truskinovsky^{2,†}

¹LMS, CNRS—UMR 7649, Ecole Polytechnique, Université Paris-Saclay, 91128 Palaiseau, France

²PMMH, CNRS—UMR 7636 PSL-ESPCI, 10 Rue Vauquelin, 75005 Paris, France

(Received 29 October 2017; revised manuscript received 12 January 2018; published 1 March 2019; corrected 13 March 2019)

A salient feature of skeletal muscles is their ability to take up an applied slack in a microsecond timescale. Behind this fast adaptation is a collective folding in a bundle of elastically interacting bistable elements. Since this interaction has a long-range character, the behavior of the system in force and length controlled ensembles is different; in particular, it can have two distinct order-disorder-type critical points. We show that the account of the disregistry between myosin and actin filaments places the elementary force-producing units of skeletal muscles close to both such critical points. The ensuing “double criticality” contributes to the system’s ability to perform robustly and suggests that the disregistry is functional.

DOI: 10.1103/PhysRevLett.122.088103

If an isometrically activated muscle is suddenly shortened, the force first abruptly decreases but then partially recovers over ~ 1 ms timescale [1–3]. Behind this swift contraction is a cooperative conformational change in an assembly of actin-bound myosin heads (cross bridges). Given that the implied “power stroke” takes place at a timescale that is much shorter than the timescale of the adenosine triphosphate (ATP)-driven attachment-detachment (~ 100 ms) [4–6], the fast force recovery can be interpreted as a *passive* phenomenon [7,8].

If it is an applied force, which is controlled, the mean-field theory of fast force recovery, viewing filaments as rigid and cross bridges as parallel [9], predicts the possibility of metastability associated with a coherent response [10]. It also predicts the existence of an order-disorder-type critical point, and it was argued that this critical point plays an essential role in the functioning of the muscle machinery [11,12]. This is consistent with the fact that critical systems are ubiquitous in biology which is explained by their adaptive advantages, in particular, their robustness in the face of random perturbations [13–17]. Criticality is often linked to marginal stability and, indeed, skeletal muscles are known to exhibit near zero rigidity in physiological (isometric contractions) conditions [2,18–20].

The mechanical functioning of the force generated system is complicated by the fact that muscle architecture involves both parallel and series connections (see Fig. 1). Parallel elements respond to a common displacement (hard device, Helmholtz ensemble), while series structures sense a common force (soft device, Gibbs ensemble). To fold coherently, individual contractile units should be able to coordinate in both types of loading conditions; however, the dominance of long-range interactions [21,22] induces *different* collective behavior in force and length controlled ensembles [10]. In particular, the critical points corresponding to length and force clamp loading conditions are strictly distinct [12].

In realistic conditions, however, they turn out to be close to each other and, to ensure the robustness of the response under a broad range of mechanical stimuli [23], the system can be poised in the vicinity of *both* critical points.

In this Letter, we argue that such double criticality is actualized in the system of muscle cross bridges due to quenched disorder. While skeletal muscles are often compared to ideal crystals, the perfect ordering is compromised by the intrinsic disregistry between the periodicities of myosin cross bridges and actin binding sites. Binding of cross bridges is restricted to incompatibly placed segments on actin filaments (target zones), and experimental studies based on electron microscopy and x-ray diffraction suggest that myosin heads are bound to actin at seemingly random positions [24,25]. To gain an insight into the role of variable offsets, we assume that the attachment sites are indeed chosen at random and show that it results in an analytically tractable model.

The idea that actomyosin disregistry brings the system’s stiffness to zero was pioneered in [26]. More recently, the utility of quenched disorder for the *active* aspects of muscle mechanics has been advocated in [27]. The beneficial role of random inhomogeneity has been established in many other fields of physics from high-temperature

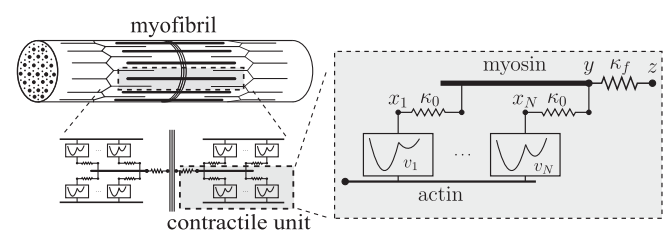


FIG. 1. Schematic representation of a muscle myofibril, of an elementary contractile unit (half-sarcomere) and of a parallel bundle of N cross bridges. In the model, the double-well potentials are mimicked by spin variables.

superconductivity in electronic materials [28] to Griffiths phases in brain networks [29].

To explore the reachability of the double-criticality in realistic conditions, we reduce the description of the system of interacting cross bridges to a random field Ising model (RFIM) and compute the equilibrium free energy applying techniques from the theory of glassy systems [30]. We then use the available experimental data on skeletal muscles to justify the claim that quenched disorder is the factor ensuring the targeted mechanical response.

We associate with each cross bridge a spin variable x taking the value 0 in the pre-power-stroke state (unfolded conformation) and -1 in the post-power-stroke state (folded conformation). Each spin element is then placed in series with a linear elastic spring of stiffness κ_0 . If we nondimensionalize lengths by the power-stroke size a and energy by $\kappa_0 a^2$, the dimensionless energy of a cross bridge reads $(1+x)v + \frac{1}{2}(y-x)^2$, where y is the dimensionless displacement of myosin relative to actin and v is the dimensionless energetic bias (see Fig. 1). To model disorder, we assume that the parameter v is different for different cross bridges [31].

Consider now a parallel bundle of N cross bridges shown schematically in Fig. 1. Individual cross bridges are attached to a backbone composed of myosin tails. The elasticity of the backbone can be accounted through a lump spring of stiffness κ_f in series with the bundle [32–34]. The system loaded in a hard device is then characterized by the dimensionless energy

$$E = \sum_{i=1}^N \left[(1+x_i)v_i + \frac{1}{2}(y-x_i)^2 \right] + N \frac{\lambda_f}{2} (z-y)^2, \quad (1)$$

where z is the applied displacement and $\lambda_f = \kappa_f / (N\kappa_0)$. We assume that the parameters v_i are independent identically distributed random variables with probability density $p(v)$.

If we replace variables x_i by $s_i = 2x_i + 1 = \pm 1$ and adiabatically eliminate y , assuming that $\partial E / \partial y = 0$, the energy (1) takes the form

$$E = -J / (2N) \sum_{i,j} s_i s_j - \sum_i h_i s_i + c,$$

where $J = 1/4(1 + \lambda_f)$, c is a z -dependent constant, and the coefficients h_i are linear in v_i (see Supplemental Material [35]). We can then conclude that (1) is a version of the mean-field RFIM, which is explicitly solvable [38,39].

Using the self-averaging property of the free energy in the thermodynamic limit, we write

$$\mathcal{F}(\beta, z) = - \lim_{N \rightarrow \infty} (N\beta)^{-1} \langle \log \mathcal{Z}(\beta, z; \{v\}) \rangle_v,$$

where the averaging $\langle \cdot \rangle_v$ is over the disorder, $\beta = \kappa_0 a^2 / (k_B T)$, and

$$\mathcal{Z} = \int dy \sum_{x \in \{0, -1\}^N} \exp(-\beta E(\mathbf{x}, y, z; \{v\})).$$

In the thermodynamic limit, we obtain [35]

$$\begin{aligned} \mathcal{F}(\beta, z) = & \frac{\lambda_f}{2} (z - y_0)^2 + \frac{1}{4} (y_0 + 1)^2 + \frac{1}{2} \left(\frac{y_0^2}{2} + v_0 \right) \\ & - \frac{1}{\beta} \int dv p(v) \log \left[2 \cosh \left(\frac{\beta}{4} (1 + 2y_0 - 2v) \right) \right], \end{aligned} \quad (2)$$

where y_0 must solve the self-consistency equation

$$y_0 = \frac{2\lambda_f z - 1}{2(\lambda_f + 1)} + \int dv \frac{p(v)}{2(\lambda_f + 1)} \tanh \left(\frac{\beta}{4} (1 - 2v + 2y_0) \right). \quad (3)$$

The multiplicity of solutions of Eq. (3) is a result of the nonconvexity of the free energy with respect to y , which is ultimately an effect of long-range interactions. This nonconvexity leads to the possibility of discontinuous tension-elongation curve $t = \partial \mathcal{F} / \partial z = \lambda_f (z - y_0)$.

If we assume that the disorder is Gaussian $p(v) = (2\pi\sigma^2)^{-1/2} \exp\{-[(v - v_0)^2 / 2\sigma^2]\}$, the behavior of the system will be fully defined by the temperature $1/\beta$, the variance of disorder σ^2 , and the parameter λ_f , characterizing the degree of elastic coupling. The resulting phase diagram is shown in Fig. 2. The disorder-free section $\sigma = 0$ of this diagram was previously studied in [12]. At $\sigma > 0$ the system responds as if it was subjected to a higher effective temperature [40,41]. The Helmholtz free energy $\mathcal{F}(\beta, z)$ and the tension-elongation relations $t(\beta, z)$ in the three phases I, II, and III are illustrated in Fig. 3.

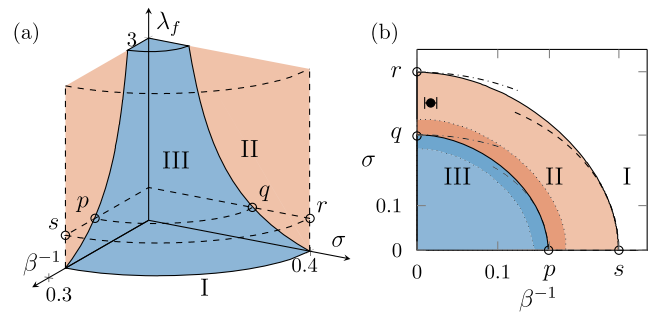


FIG. 2. (a) Configuration of phases I, II, and III in the parameter space $(1/\beta, \sigma, \lambda_f)$. (b) A section of this phase diagram corresponding to $\lambda_f = 0.54 \pm 0.2$; the shadowed region near the boundary of II and III reflects the uncertainty in λ_f . The realistic dataset for skeletal muscles is presented in (b) by a filled circle with the superimposed error bars indicating uncertainty in temperature. Analytic approximations in (b): dashed-dotted lines indicate low temperature limit; dashed lines indicate low disorder limit.

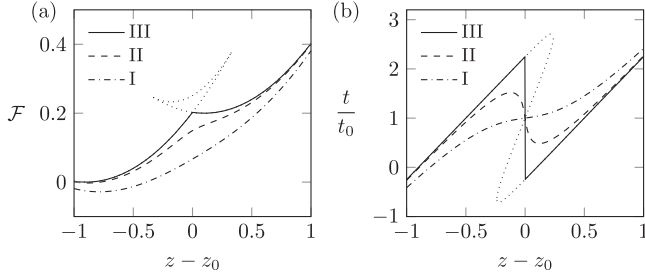


FIG. 3. (a) Representative Helmholtz free energies in each of the phases I, II, III. (b) The corresponding tension-elongation relations; $z_0 = (1 + \lambda_f)v_0/\lambda_f - 1/2$; $t_0 = v_0$.

In phase I, the cooperativity is absent and the cross bridges fluctuate independently. In phase III, the cross bridges can synchronously switch between two “pure states.” In the intermediate phase II, the tension-elongation relation exhibits negative stiffness. The boundary between phases II and III is defined by the condition $\partial^2 \tilde{\mathcal{F}}(\beta, z, y)/\partial y^2 = 0$, which means that the three roots of (3) coincide.

In the limiting case $\sigma \rightarrow 0$, the point p in Fig. 2(b) is at $\beta = 4(\lambda_f + 1)$. Around this point, the $p - q$ curve can be approximated by the low-disorder approximation $\beta_e = 4(\lambda_f + 1)$ where $\beta_e = (\beta^{-2} + \sigma^2/2)^{-1/2}$ is the inverse effective temperature [35]. In another limiting case $\beta \rightarrow \infty$, the point q can be found from the equation $\sigma = 1/\sqrt{2\pi(\lambda_f + 1)}$ and around this point the $p - q$ curve is given by the small temperature approximation $\sigma_e = 1/\sqrt{2\pi(\lambda_f + 1)}$, where $\sigma_e^2 = (\sigma^2 + 2\beta^{-2}) = 2\beta_e^{-2}$ is the variance of the effective disorder [35].

The boundary between phases II and III marks a second-order phase transition: the order parameter $\phi = N^{-1} \sum_{i=1}^N \langle s_i \rangle_\beta$, where $\langle \cdot \rangle_\beta$ is the thermal average, is double valued in phase III and single valued in phase II. To distinguish between different microscopic configurations, we also compute the Edwards-Anderson (overlap) parameter $q_{EA} = N^{-1} \sum_{i=1}^N \langle \langle s_i \rangle_\beta^2 \rangle_v$ [35]. If $q_{EA} \neq 0$ while $\phi = 0$, the pre- and post-power-stroke symmetry is broken and cross bridges may be locally frozen in either of the two states, even though such local ordering in time does not imply any spatial order. Figure 4 shows that q_{EA} is indeed different from zero in the phase II close to the $p - q$ boundary, which indicates *weakly glassy* behavior [38,39,42]. This is a hint that, in a more realistic model, where the finite backbone stiffness is taken into account, a real “strain glass” phase [43,44] may appear.

To find the boundary between phases I and II, we need to solve the equation $\partial^2 \mathcal{F}/\partial z^2 = 0$ or $\partial y_0/\partial z = 1$, where y_0 is a solution of (3). When $\sigma = 0$, we obtain $\beta = 4$, which defines the location of point s in Fig. 2(b) (see also [10,33]). The low-disorder approximation gives $\beta_e = 4$. In another limiting case $\beta \rightarrow \infty$, the location of the point r in Fig. 2(b) is given by $\sigma = \sigma_e = \sqrt{1/2\pi}$.

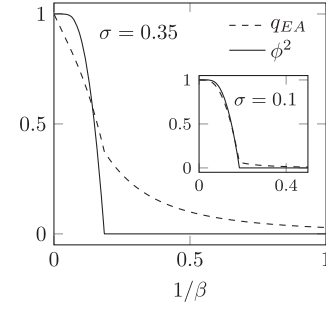


FIG. 4. The behavior of the parameter ϕ^2 (solid lines) and the Edwards-Anderson parameter q_{EA} (dashed lines) near the boundary between phases II and III at the realistic value of disorder. (Inset) The case of weak disorder.

The boundary between the phases I and II can be also interpreted as a line of second-order phase transitions, but now in the soft device (force clamp) ensemble. In this case, the presence of a series spring is irrelevant and we can assume that $\lambda_f \rightarrow 0$, $z \rightarrow \infty$, but $\lambda_f z \rightarrow t$, where tension t is the new control parameter. Following the approach used in the case of a hard device, we similarly obtain the Gibbs free energy $\mathcal{G}(\beta, t)$ and compute the tension-elongation relation $y = -\partial \mathcal{G}/\partial t$ (see Supplemental Material [35]).

In Fig. 5, we show that the soft device tension-elongation relation in phase II is monotone but discontinuous. On the boundary of I and II [see Fig. 2(b)], the stiffness becomes zero in stall conditions, which means that it is a set of critical points in the soft device ensemble. This line, targeted numerically in [26], represents regimes that can be expected to deliver the optimal trade-off between robustness and flexibility in the soft device [45,46].

So far, we have operated under an implicit assumption that in the thermodynamic limit $\kappa_f \rightarrow \infty$, while λ_f remains finite. This assumption is based on the picture of a myosin filament as a parallel arrangement of N myosin tails, all contributing to the lump stiffness of the backbone. Another limiting assumption may be that the effective stiffness of the backbone κ_f does not depend on the number of attached cross bridges N and, in this case, we have a different scaling $\lambda_f \sim N^{-1}$. Then Fig. 2(a), illustrating in this case the size effect, suggests that the quasicritical behavior can be

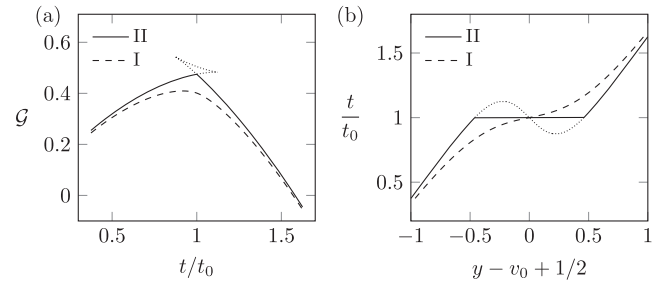


FIG. 5. (a) Representative Gibbs free energies in each of the phases I and II. (b) The corresponding tension-elongation curves; $z_0 = (1 + \lambda_f)v_0/\lambda_f - 1/2$; $t_0 = v_0$.

associated only with the particular (optimal) number of cross bridges.

To apply our results to a realistic muscle system, we use the data for *Rana temporaria* at $T = 277.15$ K [12]. From structural analysis, we obtain the value $a \sim 10$ nm [47–49]. Measurements of the fiber stiffness in *rigor mortis*, where all the 294 cross bridges per half-sarcomere were attached, produced the estimate $\kappa_0 = 2.7 \pm 0.9$ pN/nm [18,19]. The number of attached cross bridges in physiological conditions is $N = 106 \pm 11$ and experimental measurements at different N converge on the value $\kappa_f = 154 \pm 8$ pN nm⁻¹ for the lump filaments stiffness [5,50,51]. This gives $\lambda_f = 0.54 \pm 0.2$. Knowing κ_0 and a , we can estimate the nondimensional inverse temperature $\beta = 71 \pm 26$.

Now, for $y > y_*$, where $y_* = v_0 - 1/2$, the ground state of a single cross bridge is in the pre-power-stroke state, while for $y < y_*$ it is in the post-power-stroke state, so y_* represents the characteristic offset for an individual cross bridge. Knowing that $y_* \sim 4$ nm [2,26], we conclude that $v_0 \sim 24.3$ pN/($\kappa_0 a$). It was experimentally shown in [25] that at least 60% of the cross bridges are axially displaced within half of the spacing between actin monomers, which corresponds to ~ 2.76 nm shift from the nearest actin binding site (see also [26]). Given the linear relation between v_0 and y_* , with the proportionality coefficient equal to one, the variances of these two quantities are the same. If the axial offsets are Gaussian random numbers, we can estimate the standard deviation of the energetic bias $\sigma \sim 3.3$ nm/ a [35].

Based on these data we find that, rather remarkably, the system appears to be operating in a narrow domain of stability of phase II, close to both critical lines $p - q$ and $r - s$ [see the point marked by a filled circle in Fig. 2(b)]. The gap between these boundaries corresponds to ~ 1 nm difference in the cross bridge attachment positions, which is rather small given that the size of a single actin monomer is about 5.5 nm. The mechanical responses in the adjacent critical regimes are structurally similar; however, if in the hard device ensemble we can expect coherent fluctuations of *stress* (infinite rigidity), in the soft device, criticality would manifest itself through system size correlations of *strain* (zero rigidity).

The special nature of the critical regimes is illustrated in Fig. 6 for the case of a hard device. In phase I, the response is uncorrelated, and the collective power stroke is impossible [Figs. 6(a) and 6(d)]. In phase III, the response is synchronous but at the cost of crossing an energetic barrier that diverges in the thermodynamic limit (\mathcal{F} is the free energy *per* cross bridge), which facilitates freezing (metastability) in the pure states [see Figs. 6(b) and 6(e)]. The advantage of the critical regime is that the system can perform the *collective* stroke without crossing a prohibitively high macroscopic barrier, [Figs. 6(c) and 6(f)]. The analysis is similar for the case of a soft device.

Our study then suggests that evolution might have used quenched disorder to tune the muscle machinery to perform

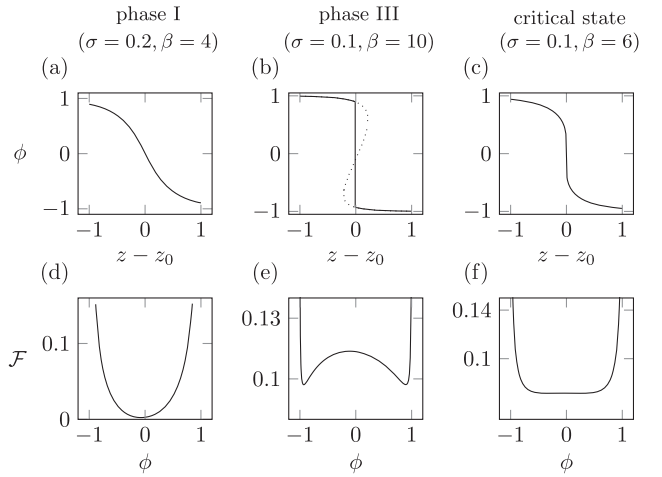


FIG. 6. The structure of the energy barriers in different regimes for the case of the hard device. (a)–(c) z dependence of the order parameter $\phi = N^{-1} \sum_{i=1}^N \langle s_i \rangle$ in different regimes; (d)–(f) matching free energies at fixed $z = z_0$, $\lambda_f = 0.35$ and $v_0 = 0.1$

near the conditions where both the Helmholtz and the Gibbs free energies are singular. Such design is highly functional when elementary force-producing units are loaded in a mixed soft-hard device. We recall that the muscle architecture is characterized by hierarchical structures with coupled modular elements loaded both in parallel and in series. In such systems, the proximity to only one of the two critical points will not be sufficient to ensure high performance in a broad range of conditions [23,52]. Moreover, as we show in the Supplemental Material [35], the very idea of ensemble independent *local* constitutive relations for such systems is questionable.

In conclusion, we established new links between muscle physiology and the theory of spin glasses and revealed a tight relation between actomyosin disregistry and the optimal mechanical performance of the force-generating machinery. At a price of neglecting many important features of actual muscles, we were able to focus attention on the role of quenched disorder in the functioning of this biological system. The observed *glassiness* in the regime of isometric contractions allows the system to access the whole spectrum of rigidities from zero (adaptability, fluidity) to infinite (control, solidity) and may serve as the factor ensuring the largest dynamic repertoire for the “muscle material.” Similar disorder-mediated tuning towards criticality can be expected in other biological systems relying on bistability and long-range interactions [9], including hair cells, which employ elastically coupled gating springs [53] and focal adhesions with their cell adhesion molecules bound to a common elastic substrate [54].

The authors thank M. Caruel and R. Garcia-Garcia for helpful discussions. H. B. R. received support from an Ecole Polytechnique Fellowship; L. T. was supported by Grant No. ANR-10-IDEX-0001-02 PSL.

- *hudson.borja-da-rocha@polytechnique.edu
†lev.truskinovsky@espci.fr
- [1] R. J. Podolsky, *Nature (London)* **188**, 666 (1960).
[2] A. F. Huxley and R. M. Simmons, *Nature (London)* **233**, 533 (1971).
[3] M. Irving, V. Lombardi, G. Piazzesi, and M. A. Ferenczi, *Nature (London)* **357**, 156 (1992).
[4] J. Howard, *Mechanics of Motor Proteins and the Cytoskeleton* (Sinauer Associates, Sunderland, Massachusetts, US, 2001).
[5] G. Piazzesi, M. Reconditi, M. Linari, L. Lucii, Y.-B. Sun, T. Narayanan, P. Boesecke, V. Lombardi, and M. Irving, *Nature (London)* **415**, 659 (2002).
[6] M. Kaya, Y. Tani, T. Washio, T. Hisada, and H. Higuchi, *Nat. Commun.* **8**, 16036 (2017).
[7] A. Vilfan and T. Duke, *Biophys. J.* **85**, 818 (2003).
[8] L. Marcucci and L. Truskinovsky, *Phys. Rev. E* **81**, 051915 (2010).
[9] M. Caruel and L. Truskinovsky, *Phys. Rev. E* **93**, 062407 (2016).
[10] M. Caruel, J.-M. Allain, and L. Truskinovsky, *Phys. Rev. Lett.* **110**, 248103 (2013).
[11] M. Caruel and L. Truskinovsky, *J. Mech. Phys. Solids* **109**, 117 (2017).
[12] M. Caruel and L. Truskinovsky, *Rep. Prog. Phys.* **81**, 036602 (2018).
[13] E. Balleza, E. R. Alvarez-Buylla, A. Chaos, S. Kauffman, I. Shmulevich, and M. Aldana, *PLoS One* **3**, e2456 (2008).
[14] J. Beggs and N. Timme, *Front. Phys.* **3**, 163 (2012).
[15] T. Mora and W. Bialek, *J. Stat. Phys.* **144**, 268 (2011).
[16] D. Krotov, J. O. Dubuis, T. Gregor, and W. Bialek, *Proc. Natl. Acad. Sci. U.S.A.* **111**, 3683 (2014).
[17] D. A. Kessler and H. Levine, arXiv:1508.02414.
[18] E. Brunello, M. Caremani, L. Melli, M. Linari, M. Fernandez-Martinez, T. Narayanan, M. Irving, G. Piazzesi, V. Lombardi, and M. Reconditi, *J. Physiol.* **592**, 3881 (2014).
[19] G. Piazzesi, M. Reconditi, M. Linari, L. Lucii, P. Bianco, E. Brunello, V. Decostre, A. Stewart, D. Gore, T. Irving, M. Irving, and V. Lombardi, *Cell* **131**, 784 (2007).
[20] M. Linari, I. Dobbie, M. Reconditi, N. Koubassova, M. Irving, G. Piazzesi, and V. Lombardi, *Biophys. J.* **74**, 2459 (1998).
[21] A. Campa, T. Dauxois, and S. Ruffo, *Phys. Rep.* **480**, 57 (2009).
[22] J. Barré, D. Mukamel, and S. Ruffo, *Phys. Rev. Lett.* **87**, 030601 (2001).
[23] M. A. Muñoz, *Rev. Mod. Phys.* **90**, 031001 (2018).
[24] R. T. Tregear, R. J. Edwards, T. C. Irving, K. J. Poole, M. C. Reedy, H. Schmitz, E. Towns-Andrews, and M. K. Reedy, *Biophys. J.* **74**, 1439 (1998).
[25] R. T. Tregear, M. C. Reedy, Y. E. Goldman, K. A. Taylor, H. Winkler, C. Franzini-Armstrong, H. Sasaki, C. Lucaveche, and M. K. Reedy, *Biophys. J.* **86**, 3009 (2004).
[26] A. F. Huxley and S. Tideswell, *J. Muscle Res. Cell Motil.* **17**, 507 (1996).
[27] P. F. Egan, J. R. Moore, A. J. Ehrlicher, D. A. Weitz, C. Schunn, J. Cagan, and P. LeDuc, *Proc. Natl. Acad. Sci. U.S.A.* **114**, E8147 (2017).
[28] J. Zaanen, *Nature (London)* **466**, 825 (2010).
[29] P. Moretti and M. A. Muñoz, *Nat. Commun.* **4**, 2521 (2013).
[30] T. Castellani and A. Cavagna, *J. Stat. Mech.* (2005) P05012.
[31] This form of the quenched disorder is equivalent to the explicit introduction of a prestrain in each of the linear springs and is also a signature of spatially inhomogeneous ATP driving.
[32] M. Linari, G. Piazzesi, and V. Lombardi, *Biophys. J.* **96**, 583 (2009).
[33] M. Caruel, J.-M. Allain, and L. Truskinovsky, *J. Mech. Phys. Solids* **76**, 237 (2015).
[34] F. Jülicher and J. Prost, *Phys. Rev. Lett.* **75**, 2618 (1995).
[35] See Supplemental Material at <http://link.aps.org/supplemental/10.1103/PhysRevLett.122.088103> for the details of the mapping on the RFIM, the computation of Helmholtz and Gibbs free energies, the description of the boundaries between phases I and II and phases II and III, the role played by the Edwards-Anderson parameter, the random representation of the axial offset, and the mechanical behavior of two half-sarcomeres in series, which also includes Refs. [36,37].
[36] I. Vilfan and R. A. Cowley, *J. Phys. C* **18**, 5055 (1985).
[37] M. Suzuki and S. Ishiwata, *Biophys. J.* **101**, 2740 (2011).
[38] T. Schneider and E. Pytte, *Phys. Rev. B* **15**, 1519 (1977).
[39] F. Krzakala, F. Ricci-Tersenghi, and L. Zdeborová, *Phys. Rev. Lett.* **104**, 207208 (2010).
[40] S. Roux, *Phys. Rev. E* **62**, 6164 (2000).
[41] A. Politi, S. Ciliberto, and R. Scorretti, *Phys. Rev. E* **66**, 026107 (2002).
[42] I. Vilfan, *Phys. Scr.* **T19B**, 585 (1987).
[43] Y. Wang, X. Ren, and K. Otsuka, *Phys. Rev. Lett.* **97**, 225703 (2006).
[44] R. Vasseur, D. Xue, Y. Zhou, W. Ettoumi, X. Ding, X. Ren, and T. Lookman, *Phys. Rev. B* **86**, 184103 (2012).
[45] S. Kauffman, *The Origins of Order: Self-Organization and Selection in Evolution* (Oxford University Press, New York, 1993).
[46] C. Darabos, M. Giacobini, M. Tomassini, P. Provero, and F. Di Cunto, in *Advances in Artificial Life. Darwin Meets von Neumann*, edited by G. Kampis, I. Karsai, and E. Szathmáry (Springer-Verlag, Berlin, Heidelberg, 2011), pp. 281–288.
[47] R. Dominguez, Y. Freyzon, K. M. Trybus, and C. Cohen, *Cell* **94**, 559 (1998).
[48] I. Rayment, W. Rypniewski, K. Schmidt-Base, R. Smith, D. Tomchick, M. Benning, D. Winkelmann, G. Wesenberg, and H. Holden, *Science* **261**, 50 (1993).
[49] I. Rayment, H. Holden, M. Whittaker, C. Yohn, M. Lorenz, K. Holmes, and R. Milligan, *Science* **261**, 58 (1993).
[50] K. Wakabayashi, Y. Sugimoto, H. Tanaka, Y. Ueno, Y. Takezawa, and Y. Amemiya, *Biophys. J.* **67**, 2422 (1994).
[51] H. Huxley, A. Stewart, H. Sosa, and T. Irving, *Biophys. J.* **67**, 2411 (1994).
[52] W. Bialek, *Rep. Prog. Phys.* **81**, 012601 (2018).
[53] V. Bormuth, J. Barral, J.-F. Joanny, F. Jülicher, and P. Martin, *Proc. Natl. Acad. Sci. U.S.A.* **111**, 7185 (2014).
[54] U. S. Schwarz and S. A. Safran, *Rev. Mod. Phys.* **85**, 1327 (2013).

Correction: An ambiguous correction requested at proof stage in the second paragraph of text was reevaluated postpublication and has been fixed.